3-2005

Effects of an impedance threshold valve upon hemodynamics in standard CPR: studies in a refined computational model

Charles F. Babbs
Purdue University, babbs@purdue.edu

Recommended Citation
Babbs, Charles F., "Effects of an impedance threshold valve upon hemodynamics in standard CPR: studies in a refined computational model" (2005). *Weldon School of Biomedical Engineering Faculty Publications.* Paper 21.
http://dx.doi.org/10.1016/j.resuscitation.2005.03.023

Effects of an impedance threshold valve upon hemodynamics in standard CPR: studies in a refined computational model

Charles F. Babbs[a,b]

[a] Department of Basic Medical Sciences, Purdue University; 1246 Lynn Hall, West Lafayette, IN 47907-1246, USA

[b] Indiana University School of Medicine, Indianapolis, IN, USA

Address for correspondence and proofs:
Charles F. Babbs, MD, PhD
1426 Lynn Hall
Purdue University
West Lafayette IN 47907-1246, USA
E-mail: babbs@purdue.edu
Voice: 765-496-2661, Fax: 765-494-0781

Revised March 10, 2005

Abstract

An impedance threshold valve (ITV) is a new airway adjunct for resuscitation that permits generation of a small vacuum in the chest during the recoil phase of chest compression.
Objectives: To explore in detail the expected magnitude and the hemodynamic mechanisms of circulatory augmentation by an ITV in standard CPR.
Method: A 14-compartment mathematical model of the human cardiopulmonary system—upgraded to include applied chest compression force, elastic recoil of the chest wall, anatomic details of the heart and lungs, and the biomechanics of mediastinal compression—is exercised to explore the conditions required for circulatory augmentation by an ITV during various modes of CPR.
Results: The ITV augments systemic perfusion pressure by about 5 mmHg compared to any particular baseline perfusion pressure without the ITV. When baseline perfusion is low, owing to either diminished chest compression force, the existence of a thoracic pump mechanism of blood flow, or the presence of an effective compression threshold, then the relative improvement produced by an ITV is significant. With an ITV the heart expands into soft pericardiac tissue, which makes the heart easier to compress.
Conclusions: An ITV can augment perfusion during CPR. The observed effectiveness of ITVs in the laboratory and in the clinic suggests a thoracic pump mechanism for standard CPR, and perhaps also an effective compression threshold that must be exceeded to generate blood flow by external chest compression.

Key words: Airway; Cardiopulmonary resuscitation (CPR); Coronary perfusion pressure; Decompression, Device; Mathematical model

1. Introduction

The impedance threshold valve (ITV) is a device that attaches to an endotracheal tube or to a ventilation mask. It allows positive pressure ventilation but prevents inspiration caused by negative pressure within the chest. When used in CPR, the inspiratory impedance valve causes negative pressures to develop within the chest during the recoil phase following each chest compression. The negative pressure is thought to enhance filling of the pump mechanism with blood and, in turn, to improve hemodynamics during CPR[1-3].

Studies in anesthetized pigs have demonstrated greater venous return and greater perfusion pressures during standard CPR when an ITV is attached to the airway[1, 4]. The device also improves the effectiveness of active compression-decompression or ACD-CPR, by preventing "decompression of the decompression"—that is by preventing an inrush of air through the trachea as the chest is actively expanded by withdrawal of a plunger device[2, 5-7]. Clinical studies suggest improved outcome when an ITV is attached to the airway during standard CPR[8-10].

The present paper describes a comprehensive study of the hemodynamic effects of an ITV in a computational model of the cardiopulmonary system that incorporates airways, lungs and 14 vascular compartments. Both external force on the chest and natural recoil of the rib cage are explicitly modeled. This model allows easy study of physiologic mechanisms of action, since pressures and flows are known everywhere in the model at every point in time. One can also compare ITV action in standard CPR of varying quality, including more or less effective methods of chest compression and more or less effective internal chest pump mechanisms.

2. Methods

To model the action of an ITV one must not only consider flow of air in the lungs and flow of blood in the vessels but also the problem of mechanical coupling of the external force on the chest to the internal pressure on the heart. This paper presents a first attempt at capturing the essence of the relevant biomechanical coupling within the chest during CPR. Variable names for the analysis are defined in Table 1. Standard values of parameters are provided in Table 2.

2.1. Depth of chest compression

To model the influence of external chest compressions and lung ventilations upon the arrested circulation in CPR, the author adopted a simplified scheme illustrated in Figure 1, in which the opposition of the chest to external compression is represented as a simple spring and damper system. Here the whole chest and rib cage are regarded mechanically as paired springs and dampers with collective spring constant, k, and damping constant, μ. These resist a known time-varying external force, F(t), on the sternum. The depression of the sternum is denoted x_1. The chambers of the heart are supported and cushioned between the sternum and the spine by soft precardiac and retrocardiac tissues having Young's modulus of elasticity, E, and resting front-to-back dimension d_0.

Motion of the sternum in response to force F(t) is given by the differential equation

$$F(t) - kx_1 - \mu\dot{x}_1 = 0, \qquad (1)$$

for sternal displacement, x_1, and velocity of displacement $\dot{x}_1$. (Here the "dot" over x_1 indicates the first time derivative.) The constants k and μ are taken from the experimental results of Gruben et al[11] for the adult human chest. With the spring constant k = 75 Nt/cm and the damping constant μ = 2.75 Nt/cm/sec this simple spring and damper model reproduces the experimentally measured force versus displacement data for the human chest[11], including hysteresis. For numerical computation it is sufficient to specify the velocity of the sternum as $\dot{x}_1 = (F(t) - kx_1)/\mu$, keeping track of the sternal position as a function of time, t, as $x_1 = \int_0^t \dot{x}_1 dt$.

2.2. Mediastinal pressure

Pressure on the heart and great vessels impels circulation in CPR. Let us denote the mediastinal pressure caused by chest compression as P_M. For simplicity let us regard the mediastinum as an elastic material for which internal stress (pressure) is related to the strain (percent compression) by a constant known as Young's modulus of elasticity, E. In particular, the pressure is equal to Young's modulus of elasticity, E, multiplied by the strain[12]. Let x_2 represent the anteroposterior expansion of a particular heart chamber such as the right ventricle due to changes in its internal blood volume. Then the pressure on the outer surface of the chamber is

$$P_M = E(x_1 + x_2)/d_0, \tag{2a}$$

and the time rate of change in external pressure on the chamber is

$$\dot{P}_M = E(\dot{x}_1 + \dot{x}_2)/d_0. \tag{2b}$$

We can solve Eq. (1) for $\dot{x}_1 = (F(t) - kx_1)/\mu$, knowing the force on the chest as a function of time, and constants k and μ. We can also know the rate of expansion, $\dot{x}_2$, of the cardiac chamber, based upon its average cross sectional area (~20 cm^2), which can be estimated from anatomy, and the inflow and outflow rates for the heart chamber, which will be known from operation of the rest of the circulatory model. In this case $\dot{x}_2 = (i_{in} - i_{out})/A_c$, where i_{in} is the rate of inflow into the cardiac chamber, i_{out} is the rate of outflow, and A_c is the characteristic cross sectional area of the chamber. The key idea is that when a particular cardiac chamber fills with blood, it encroaches on precardiac and retrocardiac tissue. The opposite effect happens when the chamber empties.

Young's modulus of elasticity for pericardiac tissues can be estimated from published biomechanical studies of the elastic properties of lung, esophagus, and loose connective tissue (Table 3). For small strains in the neighborhood of 10 to 30 percent, E can be considered constant[13]. Taking an average value of the soft tissues from Table 3, as E ~ 12,000 Pa, estimating d_0 for combined precardiac and retrocardiac tissues as 10 cm, noting 133 Pa = 1 mmHg, and substituting into Eq. 2, we can compute the external pressure on the heart in mmHg as

$$P_M \approx \frac{12000}{1330}(x_1 + x_2) \approx 9(x_1 + x_2)\ \text{mmHg}, \text{ and} \tag{3a}$$

$$\dot{P}_M \approx 9(\dot{x}_1 + \dot{x}_2)\ \text{mmHg/sec}. \tag{3b}$$

This relationship is rather credible on the basis of animal and human studies of CPR in which intrathoracic pressures have been measured in the cardiac chambers and the esophagus[14-16]. On the basis of these studies one can estimate that a 5 cm sternal depression produces a roughly 50

mmHg increase in intrathoracic pressure, which would suggest that $P_M(x_1) \approx 10\, x_1$ for x_1 in cm and P_M in mmHg, which is remarkably close to (3a).

An alternative representation of mediastinal pressure would be of the form $P_M = 9 \max(0, x - 2)$ mmHg, which incorporates the concept of an "effective compression threshold", denoted x_0 and equal to 2 cm in this example. This concept derives from one of the few studies of the influence of the magnitude of external force of compression in CPR[15]. Interestingly the first 2 cm or so of sternal compression in dogs produces no increase in esophageal pressure and no measurable blood flow or rise in mean arterial pressure. The first two cm appear to constitute a form of dead space or slack, which must be taken up before there is artificial cardiac output[15]. In this case $\dot{P}_M \approx 9(\dot{x}_1 + \dot{x}_2)$ mmHg / sec whenever $x_1 + x_2 > 2$, and $\dot{P}_M = 0$ otherwise. For most simulations to follow we shall assume an effective compression threshold of $x_0 = 2$ cm.

2.3. Lung pressure

From a mechanical viewpoint the lungs can be regarded as gas filled balloons open to air via the tracheobronchial tree. For these compartments the pressure compared to atmospheric pressure is $P_{lung} = (\Delta V_{chest} + V_{in} - V_{out})/C_{lung}$, where ΔV_{chest} is the decrease in lung volume do to chest compression in CPR, $V_{in} - V_{out}$ is the net volume added via the airways, and C_{lung} is the combined lung-chest wall compliance. Here for simplicity we do not include the net volume of blood leaving the thorax during chest compression (~20 ml), which is small compared to the lung volume change caused by chest compression (~500 ml).

The change in lung pressure over small time interval dt may be given by the expression

$$dP_{lung} = \frac{dt}{C_{lung}} \left[\dot{x}_1 A_L - \frac{(P_{lung} - P_{mouth})}{R_{airway}} \right]. \qquad (4)$$

Here $\dot{x}_1$ is the rate of sternal compression, A_L is the cross sectional area of lung influenced by chest compression (~100 cm^2), and the left hand term, $\dot{x}_1 A_L$, is the volume swept out by chest compression. The right hand term is the flow of gas out of the chest via the airways through the airway resistance. This difference, multiplied by dt, is the volume change of uncompressed lung, which when divided by lung-chest compliance, gives the corresponding pressure change, assuming that the volume change is small with respect to total lung volume.

2.4. Cardiac and thoracic pump mechanisms

In our model the cardiac ventricles experience external pressure $P_{lung} + P_M$ as a function of time. The atria, central pulmonary arteries, central pulmonary veins, and thoracic aorta experience $P_{lung} + f_{tp} P_M$ for thoracic pump factor $0 \le f_{tp} \le 1$, depending on the degree to which the "thoracic pump" mechanism of CPR is working. In this case a pressure equal to the product of P_M and f_{tp} is applied to mediastinal vascular compartments other than the right and left ventricles to create a continuum of hybrid pump mechanisms ranging from pure cardiac pump ($f_{tp} = 0$) to pure thoracic pump ($f_{tp} = 1$). When $f_{tp} = 1$ all mediastinal structures, including the great veins and thoracic aorta, experience a uniform "global" intrathoracic pressure rise, as originally conceived by Weisfeldt, Rudikoff and coworkers [17]. When $f_{tp} = 0$, only the right and left ventricules are pressurized, as in open chest CPR[18-20]. Intermediate values of the thoracic pump factor allow models approximating the current understanding[14, 21, 22], in which for small animals and children blood is impelled predominantly by the cardiac pump mechanism (for example, $f_{tp} \approx 0.25$), whereas in larger animals and adult humans blood is impelled predominantly by the thoracic pump mechanism (for example, $f_{tp} \approx 0.75$). In the present model the peripheral pulmonary arteries and veins within the lungs experience external pressure P_{lung} only.

2.5. Circulatory model

The computational model used here (Figures 2 and 3) is an adaptation of that previously published for resuscitation research by this author[23]. The number of vascular compartments is increased from 7 to 14 in order to include explicitly the anatomic details of the pulmonary circulation and a 4-chambered heart (Figure 3). The model is based upon normal human anatomy and physiology, the definition of compliance (volume change / pressure change), and Ohm's Law (flow = pressure / resistance). The model was solved using Microsoft Visual Basic to perform numerical integration of coupled differential equations describing incremental pressure changes in each vascular compartment.

2.6. Anatomical parameters

The human circulatory system is represented by 14 compliant chambers, connected by resistances through which blood may flow, as shown in Figures 2 and 3. Definitions of subscripts indicating particular vascular structures are provided in Table 1. The compliances correspond to the thoracic aorta, abdominal aorta, carotid arteries, femoral arteries, jugular veins, leg veins, right atrium and superior vena cava, right ventricle, central pulmonary arteries, peripheral pulmonary arteries, left atrium and central pulmonary veins, peripheral pulmonary veins, and left ventricle.

Conductance pathways with non-zero resistances, R, connect the vascular compartments. The values of R_h, R_{ht}, R_s and R_l are large and represent resistances of the systemic vascular beds of the head, heart, trunk, and legs. R_c, R_a, R_j, R_{ia}, R_{iv}, R_{cppa} , R_{cppv} ,and R_v are small and represent in-line resistances of the great vessels. R_{pc} is intermediate in value and represents the resistance of the pulmonary capillary bed, which is much less than that of the systemic vascular bed. Also included are the small resistances, R_{tv}, R_{pv}, R_{mv}, R_{av}, which represent the inflow and outflow resistances of the tricuspid, pulmonic, mitral, and aortic valves of the heart. Niemann's valves between the chest and jugular veins at the level of the thoracic inlet are actual, but little known anatomic structures that function to block headward transmission of large positive pressure pulses in the chest during cough and also during CPR[24].

2.7. Physiological parameters

Parameters describing a textbook normal "70 Kg man"[25] are used to specify values of the compliances and resistances in Figures 2 and 3. The normal 30-fold ratio of venous to arterial compliance characterizes a circulatory system in the absence of fluid loading or congestive heart failure. The distribution of vascular conductances (1/Resistances) into cranial, thoracic, and caudal components reflects textbook distributions of cardiac output to various body regions. Details of the rationale for selection of resistance and compliance values are provided in references[25-27]. The normal diastolic compliance of the left ventricle was taken from Greger and Windhorst's comprehensive textbook of physiology[28]. The diastolic compliance of the right ventricle was estimated as twice that of the left ventricle. The compliances pulmonary arteries and pulmonary veins are divided into central and peripheral compartments with compliances of peripheral compartments of pulmonary vessels one tenth those of the corresponding central compartments.

2.8. Solving for circulatory pressures

The relationships among the pressures in the various vascular compartments are determined by the definition of compliance and by Ohm's Law. The definition of compliance is $C = \Delta V / \Delta P$, where C is compliance, and ΔP is the incremental change in pressure across the wall of a compartment as volume ΔV is introduced. Ohm's Law, which relates flow to pressure and resistance, is $i = (P_1 - P_2)/R$, where $P_1 - P_2$ is the instantaneous difference in pressure across

resistance R as flow i occurs. In Figure 2 currents i_c (carotid), i_a (aortic), i_s (systemic), i_v (venous), i_j (jugular), i_{ia} (iliac artery), i_l (legs), i_{iv} (iliac veins), i_i (pump input), and i_o (pump output) are shown for clarity, with positive directions specified by arrows. In Figure 3 flows across each heart valve and the pulmonary vascular resistance are shown.

2.8.1. Systemic vascular components

Applying these basic concepts with reference to Figures 2 and 3 provides a set of governing finite difference equations that can be used to describe hemodynamics. These equations are integrated numerically to describe instantaneous pressure vs. time waveforms in each compartment. Beginning, for example, with the abdominal aorta

$$\Delta V_{aa} = (i_a - i_s - i_{ia})\Delta t = \left[\frac{P_{ao} - P_{aa}}{R_a} - \frac{P_{aa} - P_{ivc}}{R_s} - \frac{P_{aa} - P_{fa}}{R_{ia}} \right] \Delta t \text{ , and}$$

$$\Delta P_{aa} = \Delta V_{aa} / C_{aa} . \tag{5}$$

The term ΔV_{aa} represents the increase in abdominal aortic volume caused by net inflow of blood during the small time interval Δt. Substitution for currents, i_a , i_s , and i_{ia}, using Ohm's Law allows calculation of ΔV_{aa} from prevailing pressures.

Similarly, the pressure changes in other systemic vascular compartments are given by expressions (6) through (10), as follows.

$$\Delta V_{ivc} = (i_s - i_v + i_{fv})\Delta t = \left[\frac{P_{aa} - P_{ivc}}{R_s} - \frac{P_{ivc} - P_{ra}}{R_v} + \max\left(0 , \frac{P_{fv} - P_{ivc}}{R_{iv}} \right) \right] \Delta t$$

and

$$\Delta P_{ivc} = \Delta V_{ivc} / C_{ivc} . \tag{6}$$

In (6) the max() function is used to represent the action of venous valves in the femoral and iliac veins that prevent retrograde flow. Similarly,

$$\Delta P_{car} = \frac{1}{C_{car}} (i_c - i_h)\Delta t = \frac{\Delta t}{C_{car}} \left[\frac{P_{ao} - P_{car}}{R_c} - \frac{P_{car} - P_{jug}}{R_h} \right] \tag{7}$$

$$\Delta P_{jug} = \frac{1}{C_{jug}} (i_h - i_j)\Delta t = \frac{\Delta t}{C_{jug}} \left[\frac{P_{car} - P_{jug}}{R_h} - \max\left(0 , \frac{P_{jug} - P_{ra}}{R_j} \right) \right], \tag{8}$$

where the max() function is used in expression (8) to implement the one-way valve action of Niemann's valves during cough or intrathoracic pressure pulses (when $P_{ra} > P_{jug}$).

The legs are represented as follows.

$$\Delta P_{fa} = \frac{1}{C_{fa}}(i_{ia} - i_l)\Delta t = \frac{\Delta t}{C_{fa}}\left[\frac{P_{aa} - P_{fa}}{R_{ia}} - \frac{P_{fa} - P_{fv}}{R_l}\right] \tag{9}$$

$$\Delta P_{fv} = \frac{1}{C_{fv}}(i_l - i_{fv})\Delta t = \frac{\Delta t}{C_{fv}}\left[\frac{P_{fa} - P_{fv}}{R_l} - \max\left(0\,,\,\frac{P_{fv} - P_{ivc}}{R_{iv}}\right)\right]. \tag{10}$$

For the peripheral pulmonary arteries

$$\Delta P_{ppa} = \Delta P_{lung} + \frac{\Delta t}{C_{ppa}}(i_3 - i_4) = \Delta P_{lung} + \frac{\Delta t}{C_{ppa}}\left[\frac{P_{pa} - P_{ppa}}{R_{cppa}} - \frac{P_{ppa} - P_{ppv}}{R_{pc}}\right]. \tag{11}$$

For the peripheral pulmonary veins

$$\Delta P_{ppv} = \Delta P_{lung} + \frac{\Delta t}{C_{ppv}}(i_4 - i_5) = \Delta P_{lung} + \frac{\Delta t}{C_{ppv}}\left[\frac{P_{ppa} - P_{ppv}}{R_{pc}} - \frac{P_{ppv} - P_{la}}{R_{cppv}}\right]. \tag{12}$$

2.8.2. Chest pump components

For the thoracic aorta

$$\Delta V_{ao} = (i_o - i_c - i_a - i_{ht})\Delta t = \left[\max\left(0\,,\,\frac{P_{lv} - P_{ao}}{R_{av}}\right) - \frac{P_{ao} - P_{car}}{R_c} - \frac{P_{ao} - P_{aa}}{R_a} - \frac{P_{ao} - P_{ra}}{R_{ht}}\right]\Delta t$$

and

$$\Delta P_{ao} = \Delta P_{lung} + \frac{\Delta V_{ao}}{C_{ao}} + f_{tp}\frac{E}{d_0}\dot{x}_1\Delta t\ , \tag{13}$$

where f_{tp} is the thoracic pump factor. The rate of change in the diameter of the thoracic aorta is negligible with respect to $\dot{x}_1$ and so is omitted from Eq. 13.

For the central pulmonary arteries

$$\Delta V_{pa} = (i_2 - i_3)\Delta t = \left[\max\left(0\,,\, \frac{P_{rv} - P_{pa}}{R_{pv}}\right) - \frac{P_{pa} - P_{ppa}}{R_{cppa}} \right] \Delta t \quad , \quad \text{and}$$

$$\Delta P_{pa} = \Delta P_{lung} + \frac{\Delta V_{pa}}{C_{pa}} + f_{tp} \frac{E}{d_0} \dot{x}_1 \Delta t \quad . \tag{14}$$

Corresponding expressions for the four chambers of the heart including the right and left ventricles and the right and left atria with their associated large veins (superior vena cava and central pulmonary veins) are computed from the sum of the mediastinal pressure and lung pressure acting on the chambers and the change in internal volume divided by chamber compliance. For these large, valved cardiac chambers $i_{in} \neq i_{out}$, and therefore $\dot{x}_2$ is not negligible.

Thus for the superior vena cava and right atrium

$$\Delta V_{ra} = (i_j + i_v + i_{ht} - i_i)\Delta t$$

$$= \left[\max\left(0\,,\, \frac{P_{jug} - P_{ra}}{R_j}\right) + \frac{P_{ivc} - P_{ra}}{R_v} + \frac{P_{ao} - P_{ra}}{R_{ht}} - \max\left(0\,,\, \frac{P_{ra} - P_{rv}}{R_{tv}}\right) \right] \Delta t \quad ,$$

where the max() functions indicate the actions of Niemann's valves and the tricuspid valve. In turn,

$$\Delta P_{ra} = \Delta P_{lung} + \frac{\Delta V_{ra}}{C_{ra}} + f_{tp} \frac{E}{d_0} \left(\dot{x}_1 \Delta t + \frac{\Delta V_{ra}}{A_{ra}} \right) . \tag{15}$$

For the right ventricle

$$\Delta V_{rv} = (i_i - i_2)\Delta t = \left[\max\left(0\,,\, \frac{P_{ra} - P_{rv}}{R_{tv}}\right) - \max\left(0\,,\, \frac{P_{rv} - P_{pa}}{R_{pv}}\right) \right] \Delta t \quad ,$$

and

$$\Delta P_{rv} = \Delta P_{lung} + \frac{\Delta V_{rv}}{C_{rv}} + \frac{E}{d_0} \left(\dot{x}_1 \Delta t + \frac{\Delta V_{rv}}{A_{rv}} \right) . \tag{16}$$

For the left atrium and central pulmonary veins

$$\Delta V_{la} = \left[\frac{P_{ppv} - P_{la}}{R_{cppv}} - \max\left(0 , \frac{P_{la} - P_{lv}}{R_{mv}} \right) \right] \Delta t ,$$

$$\Delta P_{la} = \Delta P_{lung} + \frac{\Delta V_{la}}{C_{la}} + f_{tp} \frac{E}{d_0} \left(\dot{x}_1 \Delta t + \frac{\Delta V_{la}}{A_{la}} \right) . \tag{17}$$

Finally, for the left ventricle

$$\Delta V_{lv} = (i_6 - i_o)\Delta t = \left[\max\left(0 , \frac{P_{la} - P_{lv}}{R_{mv}} \right) - \max\left(0 , \frac{P_{lv} - P_{ao}}{R_{av}} \right) \right] \Delta t ,$$

$$\Delta P_{lv} = \Delta P_{lung} + \frac{\Delta V_{lv}}{C_{lv}} + \frac{E}{d_0} \left(\dot{x}_1 \Delta t + \frac{\Delta V_{lv}}{A_{lv}} \right) . \tag{18}$$

2.9. Numerical methods

2.9.1. Integration

The Visual Basic programming language and Microsoft Excel spreadsheets are ideal for implementing numerical integration of expressions (4) through (18) to obtain pressures in the lungs and in all 14 vascular compartments as a function of time. One can create a Visual Basic procedure, in which pressures in each compartment at any point in time are computed from the pressures at the preceding time point and the corresponding ΔP's—that is

$$P(t + \Delta t) = P(t) + \Delta P(t) \quad (19)$$

To model a cardiac arrest and CPR one begins with a uniform pressure such as 5 mmHg in all compartments of the arrested circulation and applies periodic force F(t) externally to the chest. To model the normal circulation as a control, one applies pressures to the cardiac ventricles only. The incremental changes in compartment pressures computed from expressions (4) through (18) are used to construct a marching solution for successive small increments of time, Δt, typically 0.00005 sec. Use of a time increment that is too coarse results in unstable oscillations of computed pressures. Decreasing the value of Δt, however, can always return stability. Smaller values of Δt are needed when a nonzero effective compression threshold is used.

2.9.2. Pressure waveforms applied to vessels in the chest and abdomen

The input parameter $F_{max\text{-}chest}$ represents peak external force applied to the sternum. In this study half sinusoidal waveforms were used. Chest force was varied from 0 to 600 Nt. A reference value of 400 Nt provided 5.1 cm chest depression at a frequency of 80 compressions/min.

2.9.3. Impedance threshold valve effect

To model the functionality of an inspiratory impedance valve, tracheal airflow was set to zero under the following conditions: ambient pressure = 0 and lung pressure < 0. This restriction permitted ordinary positive pressure rescue ventilation and exhalation under any circumstances, as is true for an active ITV.

2.9.4. Model output

The output of the model is a multi-channel record of pressure as a function of time. Standard "normal" values of model parameters are given in Table 2 and in references[26, 27]. Because of the high venous pressures that can occur during CPR or external pulsation, systemic perfusion pressure (mean thoracic aortic pressure minus mean right atrial pressure) is considered to be the most relevant pressure to describe hemodynamic benefit[29]. Hence mean systemic perfusion

pressure is the figure of merit used in the present study. It was computed for the 19th and 20th compression cycles after onset of CPR to allow steady state conditions to develop.

2.9.5. Test cases and validation

The spreadsheet code was validated by solving simple test cases for very small or very large values of the resistances and compliances and by establishing a model of the normal adult circulation using normal right and left ventricular pressures with $f_{tp} = 0$. This model had an aortic blood pressure of 117/80 mmHg and a cardiac output of 5.1 L/min for a heart rate of 80/min, closely approximating the textbook normal values of 120/80 mmHg and 5.0 L/min.

3. Results

The pressure vs. time tracings in Figures 4(a) and 4(b) show the basic effects of the ITV in standard thoracic pump CPR. The top traces are thoracic aortic pressure; the middle traces are right atrial pressure, and the bottom traces are lung pressure. The ITV lowers pulmonary pressures as expected, and systemic perfusion pressure is increased.

The effects of the ITV upon filling of the right ventricle are illustrated in Figure 4(c), which shows changes in the dorsal-ventral diameter of the right ventricle, compared to the initial no-flow state, as a function of time. The bottom trace corresponds to standard CPR; the top trace corresponds to standard CPR with the impedance threshold valve. In each case emptying occurs during early compression, and filling occurs during relaxation. During each compression cycle the rate of filling (slope of curve) during chest recoil is increased by the ITV. In addition the average steady-state diameter of the right ventricle is increased by approximately 0.4 cm. With reference to Figure 1 one may hypothesize that the steady-state dilation of the heart caused by reduced lung pressures pre-compresses pericardiac soft tissues so that greater mediastinal pressure is generated by a given sternal deflection.

To test this hypothesis one can re-run the model so that the contribution of cardiac chamber expansion to mediastinal pressure on the heart is eliminated. Specifically, one can set the variables x_2 and $\dot{x}_2$ in Equations (2) and (3) to zero. When this is done the beneficial effect of the ITV on systemic perfusion pressure is largely eliminated: systemic perfusion pressure increases from 10.6 to 10.9 mmHg only. When the effects of heart expansion are included using normal values of x_2 and $\dot{x}_2$ in Equations (2) and (3) the beneficial effect of the ITV returns, and the systemic perfusion pressure increases from 11.4 to 16.3 mmHg. Thus the ITV improves coupling of the heart to mediastinal soft tissues in standard CPR.

Figure 5 shows the effect of an ITV during standard CPR (80 compressions/min) at various levels peak chest compression force. The ITV improves systemic perfusion at all forces, but the relative difference is greater for lower forces. The displacement of the +ITV curve to the left reflects overall dilation of the heart, that is, increased average volume and diameter, which reduces the effective compression threshold. The relative improvement with an ITV is most dramatic when perfusion from standard CPR is low.

The results in Figures 4 and 5 were obtained with a thoracic pump factor of 1.0. The effect of the ITV in standard CPR is also dependent upon the chest pump mechanism, as shown in Figure 6. The absolute effect of the ITV is relatively constant, however the percent improvement in perfusion pressure is obviously greater for thoracic pump factors closer to 1.0 than for thoracic pump factors closer to zero. Figure 7 shows a similar pattern for the effective chest compression threshold, x_0. The ratio of systemic perfusion pressure with an ITV to that without an ITV increases as x_0 increases. In the presence of a nonzero effective compression threshold the heart is compressed for a longer time and with a greater pressure when it is better filled and expands into the lung tissue surrounding the heart. In this sense chest compression during CPR is more efficient for a larger heart size.

4. Discussion

Given the extreme practical difficulties of working with human or animal models of cardiac arrest and CPR, computer models have found a niche in resuscitation research[30, 31]. Such models are independent of many confounding factors present in laboratory studies and in clinical trials. These include varying patient populations, cardiac arrest time, drug therapy, underlying disease, chest configuration, and body size, as well as varying rescuer size, skill, strength, consistency, prior training, and bias. Mathematical models also allow exact control of the dominant hemodynamic mechanism of CPR (thoracic pump in large subjects, vs. cardiac pump in small subjects[26, 32]) and are especially suited to study of hemodynamic mechanisms because pressures, flows and other properties can be measured anywhere in the circulation, and there is no deterioration of the model between trials. A new feature of the model described here is the explicit representation of the biomechanical coupling between the external force on the chest and the resulting pressures developed within the cardiac chambers and great vessels.

The mechanical role of pericardiac tissues is critical to the mechanism of circulatory enhancement by the ITV. In particular, the efficacy of an ITV in standard CPR is related to increased pre-compression volumes of the cardiac ventricles and the resulting increased tension in pericardiac tissues, which in turn transmit greater force from sternal compression to the heart.

The absolute effect of the ITV on systemic perfusion pressure is rather constant. However the relative effect depends upon the baseline or control perfusion for standard CPR, which is determined by the chest compression force, the chest pump mechanism, the presence of an effective chest compression threshold, and other factors. Biologically significant augmentation of the circulation in standard CPR by an ITV is now well documented in animal models and in human patients[2]. For example, Aufderheide et al[8] and Thayne et al[10] found application of active

vs. sham ITV's roughly doubled immediate and 24 hour survival rates in patients suffering cardiac arrest. Pirrallo and Aufderheide studied invasively measured arterial blood pressure during CPR in patients suffering out-of hospital cardiac arrest. They found that estimated mean arterial pressure (diastolic + one third of pulse pressure) was 29 mmHg with sham ITV's versus 44 mmHg with active ITV's. The roughly 50 percent improvement, when combined with the present simulations, suggests that conditions favoring poor perfusion in standard CPR prevail in vivo.

The classical studies of Redding[33, 34], Ralston[35, 36], and Kern[29] all clearly show that adequate systemic perfusion pressure is critical for resuscitation success. In particular, a systemic perfusion pressure > 25 mmHg predicts survival and a systemic perfusion pressure less than 20 mmHg predicts failure to resuscitate. Thus modest increases in systemic perfusion pressure can make a critical difference. Further, the clinical studies of Sack and coworkers with interposed abdominal compression CPR[37] show that increased short-term survival can translate into increased long-term survival in a general population of persons with cardiac arrest. In particular, Sack's studies show a doubling of survival with methods known to roughly double flow. The ability of the ITV to improve systemic perfusion pressure with a trivial modification of CPR protocols (placing a valve on an endotracheal tube) appears to offer potential benefit and nearly zero risk.

The only potential downside to the ITV is increased wall tension in the myocardium associated with the roughly 0.4 cm increase in ventricular diameter. If this extra wall tension were to significantly reduce coronary circulation, then resuscitation success could be compromised. However, the animal studies of Lurie et al[1] found increased, rather than decreased, regional blood flow to the myocardium with an active ITV. These data would imply that the increased in systemic perfusion pressure is greater than any increase in coronary vascular resistance. Moreover, an analytical calculation by the present author based on formulas for coronary arteriolar resistance and compliance (details not shown) predicts only a 3 to 5 percent increase in coronary vascular resistance after a typical 10 ml increase in ventricular volume caused by an ITV. Thus the improvement in systemic perfusion pressure is greater than the increase in coronary vascular resistance after placement of an ITV in CPR.

One alternative way to overcome sluggish filling of the chest pump during CPR is the application of interposed abdominal compressions with IAC-CPR[37-39]. This strategy forces blood into the chest from the abdomen and can be quite effective, since it is easier to generate a given positive pressure in the abdomen just by pushing on it, than to generate an equivalent negative pressure in the chest. From a hemodynamic standpoint the results on the venous side are similar, and there is the added benefit of abdominal aortic counterpulsation with IAC, which tends to boost total output and perfusion of the heart and brain[40-42].

For those committed to standard CPR, the ITV is a convenient, simple, and effective means to augment circulation during cardiac arrest, chest compression, and positive pressure rescue breathing. The fact that the ITV works rather dramatically in clinical studies of standard CPR[8, 10] implies the existence of a thoracic pump mechanism and an effective compression threshold in human beings. These, in turn, emphasize the critical importance of adequate chest compression force, which can be quite variable among rescuers and can diminish gradually as a given rescuer

tires. Improved understanding of the action of the ITV in standard CPR not only justifies the use of ITV's themselves but also argues for improved training of lay and professional rescuers and in prolonged cardiac arrests the use of mechanical devices for chest compression that never tire.

References

1. Lurie KG, Voelckel WG, Zielinski T, et al. Improving standard cardiopulmonary resuscitation with an inspiratory impedance threshold valve in a porcine model of cardiac arrest. Anesth Analg 2001; 93:649-55.
2. Lurie K, Voelckel W, Plaisance P, et al. Use of an inspiratory impedance threshold valve during cardiopulmonary resuscitation: a progress report. Resuscitation 2000; 44:219-30.
3. Lurie KG, Coffeen P, Shultz J, McKnite S, Detloff B, Mulligan K. Improving active compression-decompression cardiopulmonary resuscitation with an inspiratory impedance valve. Circulation 1995; 91:1629-32.
4. Lurie KG, Zielinski T, McKnite S, Aufderheide T, Voelckel W. Use of an inspiratory impedance valve improves neurologically intact survival in a porcine model of ventricular fibrillation. Circulation 2002; 105:124-9.
5. Plaisance P, Lurie KG, Payen D. Inspiratory impedance during active compression-decompression cardiopulmonary resuscitation: a randomized evaluation in patients in cardiac arrest. Circulation 2000; 101:989-94.
6. Plaisance P, Lurie KG, Vicaut E, et al. Evaluation of an impedance threshold device in patients receiving active compression-decompression cardiopulmonary resuscitation for out of hospital cardiac arrest. Resuscitation 2004; 61:265-71.
7. Wolcke BB, Mauer DK, Schoefmann MF, et al. Comparison of standard cardiopulmonary resuscitation versus the combination of active compression-decompression cardiopulmonary resuscitation and an inspiratory impedance threshold device for out-of-hospital cardiac arrest. Circulation 2003; 108:2201-5.
8. Aufderheide TP, Pirrallo RG, Provo TA, Lurie KG. Clinical evaluation of an inspiratory impedance threshold device during standard cardiopulmonary resuscitation. Circulation 2004; 110 (Suppl III):III-413.
9. Pirrallo RG, Aufderheide TP, Provo TA, Lurie KG. An impedance threshold device significantly increases invasively measured arterial pressures during standard cardiopulmonary resuscitation in out-of-hospital cardiac arrest. Circulation 2004; 110 (Suppl III):III-414.
10. Thayne RC, vanDellen A, Thomas DC, Neville JD. An impedance threshold device improves short-term outcomes following out-of-hospital cardiac arrest. Circulation 2004; 110 (Suppl III):III-414-15.
11. Gruben KG, Guerci AD, Popel AS, Tsitlik JE. Sternal force-displacement relationship during cardiopulmonary resuscitation. Journal of Biomechanical Engineering 1993; 115:195-201.
12. Brekhovskikh LM, Goncharov V. Mechanics of Continua and Wave Dynamics. Berlin: Springer-Verlag, 1994.
13. Fung YC. Biomechanics : mechanical properties of living tissues. New York: Springer-Verlag, 1981:23-57.

14. Paradis NA, Martin GB, Goetting MG, et al. Simultaneous aortic, jugular bulb, and right atrial pressures during cardiopulmonary resuscitation in humans: Insights into mechanisms. Circulation 1989; 80:361-8.
15. Babbs CF, Voorhees WD, Fitzgerald KR, Holmes HR, Geddes LA. Relationship of artificial cardiac output to chest compression amplitude--evidence for an effective compression threshold. Annals of Emergency Medicine 1983; 12:527-532.
16. DelGuercio L, Feins NR, Cohn JD, Coomaraswamy RP, Wollman SB, State D. Comparison of blood flow during external and internal cardiac massage in man, Circulation 31(Suppl I), 1965.
17. Rudikoff MT, Maughan WL, Effron M, Freund P, Weisfeldt ML. Mechanisms of blood flow during cardiopulmonary resuscitation. Circulation 1980; 61:345-352.
18. Weiser FM, Adler LN, Kuhn LA. Hemodynamic effects of closed and open chest cardiac resuscitation in normal dogs and those with acute myocardial infarction, Am J Cardiol, 1962. Vol. 10.
19. Sanders AB, Kern KB, Ewy GA, Atlas M, Bailey L. Improved resuscitation from cardiac arrest with open chest massage, Annal Emerg Med 13, 1984.
20. Babbs CF. Hemodynamic mechanisms in CPR: a theoretical rationale for resuscitative thoracotomy in non-traumatic cardiac arrest. Resuscitation 1987; 15:37-50.
21. Halperin HR, Tsitlik JE, Guerci AD, et al. Determinants of blood flow to vital organs during cardiopulmonary resuscitation in dogs. Circulation 1986; 73:539-50.
22. Chandra NC. Mechanisms of blood flow during CPR. Ann Emerg Med 1993; 22:281-8.
23. Babbs CF. CPR techniques that combine chest and abdominal compression and decompression : Hemodynamic insights from a spreadsheet model. Circulation 1999; 100:2146-2152.
24. Niemann JT, Ung S, Rosborough JP, Suzuki J, Criley JM. Preferential brachiocephalic flow during CPR--a hemodynamic explanation. Circulation 64(IV) 1981:303.
25. Hamilton(Section-Editor) WF, Dow(Executive-Editor) P. Handbook of Physiology Volume 2, Section 2: Circulation: American Physiological Society, Washington D.C., 1963:93-95.
26. Babbs CF, Weaver JC, Ralston SH, Geddes LA. Cardiac, thoracic, and abdominal pump mechanisms in cardiopulmonary resuscitation: studies in an electrical model of the circulation. Am J Emerg Med 1984; 2:299-308.
27. Babbs CF, Ralston SH, Geddes LA. Theoretical advantages of abdominal counterpulsation in CPR as demonstrated in a simple electrical model of the circulation. Annals of Emergency Medicine 1984; 13:660-671.
28. Antoni H. Functional Properties of the Heart. In: Greger R, ed. Comprehensive Human Physiology. Vol. 2. Berlin, Heidelberg: Springer-Verlag, 1996:1801-1823.
29. Kern KB, Ewy GA, Voorhees WD, Babbs CF, Tacker WA. Myocardial perfusion pressure: a predictor of 24-hour survival during prolonged cardiac arrest in dogs. Resuscitation 1988; 16:241-250.
30. Babbs CF. Circulatory adjuncts. Newer methods of cardiopulmonary resuscitation. Cardiol Clin 2002; 20:37-59.
31. Christenson JM. Cardiopulmonary resuscitation research models: motherboards, mammals, and man. Acad Emerg Med 1995; 2:669-71.
32. Babbs CF. New versus old theories of blood flow during cardiopulmonary resuscitation. Critical Care Medicine 1980; 8:191-195.

33. Pearson JW, Redding JS. Influence of peripheral vascular tone on cardiac resuscitation. Anesth Analg 1965; 44:746-752.
34. Redding JS. Abdominal compression in cardiopulmonary resuscitation. Anesthesia and Analgesia 1971; 50:668-675.
35. Ralston SH, Voorhees WD, Babbs CF. Intrapulmonary epinephrine during cardiopulmonary resuscitation: Improved regional blood flow and resuscitation in dogs. Annals of Emergency Medicine 1984; 13:79-86.
36. Ralston SH, Showen L, Carter A, Tacker WA. Comparison of endotracheal and intravenous epinephrine dosage during CPR in dogs. Annals of Emergency Medicine 1985; 14:494-495.
37. Sack JB, Kesselbrenner MB, Bregman D. Survival from in-hospital cardiac arrest with interposed abdominal counterpulsation during cardiopulmonary resuscitation. JAMA 1992; 267:379-385.
38. Ralston SH, Babbs CF, Niebauer MJ. Cardiopulmonary resuscitation with interposed abdominal compression in dogs. Anesthesia and Analgesia 1982; 61:645-651.
39. Sack JB, Kesselbrenner MB. Hemodynamics, survival benefits, and complications of interposed abdominal compression during cardiopulmonary resuscitation. Acad Emerg Med 1994; 1:490-497.
40. Voorhees WD, Ralston SH, Babbs CF. Regional blood flow during cardiopulmonary resuscitation with abdominal counterpulsation in dogs. Am J Emerg Med 1984; 2:123-8.
41. Voorhees WD, Niebauer MJ, Babbs CF. Improved oxygen delivery during cardiopulmonary resuscitation with interposed abdominal compressions. Annals of Emergency Medicine 1983; 12:128-135.
42. Walker JW, Bruestle JC, White BC, Evans AT, Indreri R, Bialek H. Perfusion of the cerebral cortex using abdominal counterpulsation during CPR. Am J Emerg Med 1984; 2:391-393.
43. Goyal RK, Biancani P, Phillips A, Spiro HM. Mechanical properties of the esophageal wall. J Clin Invest 1971; 50:1456-65.
44. Takeda T, Kassab G, Liu J, Puckett JL, Mittal RR, Mittal RK. A novel ultrasound technique to study the biomechanics of the human esophagus in vivo. Am J Physiol Gastrointest Liver Physiol 2002; 282:G785-93.
45. Fan Y, Gregersen H, Kassab GS. A two-layered mechanical model of the rat esophagus. Experiment and theory. Biomed Eng Online 2004; 3:40.
46. Matthews FL, West JB. Finite element displacement analysis of a lung. J Biomech 1972; 5:591-600.
47. Hoppin FG, Jr., Lee GC, Dawson SV. Properties of lung parenchyma in distortion. J Appl Physiol 1975; 39:742-51.
48. Lai-Fook SJ, Wilson TA, Hyatt RE, Rodarte JR. Elastic constants of inflated lobes of dog lungs. J Appl Physiol 1976; 40:508-13.
49. Karakaplan AD, Bieniek MP, Skalak R. A mathematical model of lung parenchyma. J Biomech Eng 1980; 102:124-36.
50. Barbenel JC, Evans JH, Finlay JB. Stress-strain-time relations for soft connective tissuese. In: Kenedi RM, ed. Perspectives in Biomedical Engineering. Baltimore: University Park Press, 1973:165-172.
51. Tong P, Fung YC. The stress-strain relationship for the skin. J Biomech 1976; 9:649-57.

52. Chu BM, Frasher WG, Wayland H. Hysteretic behavior of soft living animal tissue. Ann Biomed Eng 1972; 1:182-203.
53. Patel DJ, Schilder DP, Mallos AJ. Mechanical properties and dimensions of the major pulmonary arteries. J Appl Physiol 1960; 15:92-6.

Table 1: Nomenclature

Symbol	Definition
Subscripts	
aa	Abdominal aorta
a	Aorta at level of diaphragm
ao	Thoracic aorta
av	Aortic valve
C, car	Carotid
cppa	Central to peripheral pulmonary arteries
cppv	Central to peripheral pulmonary veins
fa	Femoral artery
fv	Femoral vein
h	Head
ht	Heart
ia	Iliac artery
iv	Iliac vein
ivc	Inferior vena cava
j, jug	Jugular
L	Lungs
l	Legs
la	Left atrium and central pulmonary veins
lv	Left ventricle
M	Mediastinum
mv	Mitral valve
pa	Pulmonary arteries (central)
pc	Pulmonary capillaries
ppa	Peripheral pulmonary arteries
ppv	Peripheral pulmonary veins
pv	Pulmonic valve
ra	Right atrium and superior vena cava
s	Systemic circulation below diaphragm
tv	Tricuspid valve
v	Portal and systemic veins at level of diaphragm

(Table 1 continued)

Variables

A	Cross sectional area (cm^2)
C	Compliance (L/mmHg or ml/mmHg)
d_0	Resting front to back dimension of mediastinal soft tissues (cm)
E	Young's modulus of elasticity (Pa or mmHg)
$F(t)$	External force applied to chest over time
f_{tp}	Thoracic pump factor (0 – 1)
i	Flow or current between compartments (L/sec or L/min)
k	Spring constant of chest (Nt/cm)
μ	Damping constant of chest (Nt/cm/sec)
P	Instantaneous pressure in a compartment (mmHg)
ΔP	Pressure increment during time Δt (mmHg)
R	Resistance (mmHg/(L/sec))
t	Time during a cycle of CPR (sec)
Δt	Time increment (sec)
V	Volume (ml)
x_0	Effective compression threshold (cm)
x_1	Sternal compression (cm)
$\dot{x}_1$	Rate of sternal compression (cm/sec)
x_2	Heart chamber expansion (cm)
$\dot{x}_2$	Rate of heart chamber expansion (cm/sec)

Table 2: Model parameters

Resistances (>0)

	Value (mmHg/L/sec)	Definition
Rc	60	Resistance of both carotid arteries
Rh	5520	Resistance of the head vasculature
Rj	30	Resistance of both jugular veins
Rtv	5	Resistance of the tricuspid valve
Rpv	10	Resistance of the pulmonic valve
Rcppa	10	Resistance between central and peripheral pulmonary arteries
Rcppv	5	Resistance between central and peripheral pulmonary veins
Rmv	5	Resistance of the mitral valve
Rav	10	Resistance of the aortic valve
Rpc	105	Resistance of the pulmonary capillary bed
Rht	15780	Resistance of coronary vessels (heart)
Ra	25	Resistance of the aorta
Rv	25	Resistance of the inferior vena cava
Rs	1800	Resistance of residual systemic vasculature
Ria	360	Resistance of both iliac arteries
Riv	180	Resistance of both iliac veins
Rl	8520	Resistance of leg vasculature
Rairway	1.2	Resistance of airways to ventilation

Compliances (>0)

	Value (L/mmHg)	Definition
Crv	0.016	Compliance of the arrested right ventricle
Cpa	0.0042	Compliance of the large pulmonary arteries
Cppa	0.0042	Compliance of peripheral pulmonary arteries
Cppv	0.00128	Compliance of peripheral pulmonary veins
Cla	0.0128	Compliance of the left atrium and central pulmonary veins
Clv	0.008	Compliance of the arrested left ventricle
Ccar	0.0002	Compliance of both carotid arteries
Cjug	0.012	Compliance of both jugular veins
Cao	0.0008	Compliance of the thoracic aorta
Crh	0.0095	Compliance of the right atrium and intrathoracic great veins
Caa	0.0004	Compliance of the abdominal aorta
Civc	0.0234	Compliance of the inferior vena cava
Cfa	0.0002	Compliance of both femoral arteries
Cfv	0.0047	Compliance of both femoral veins

Other variables

	Value and units	Definition
A_L	100 cm^2	Cross section of lung squeezed by sternal compression
A_{ra} A_{la} A_{rv} A_{lv}	20 cm^2	Cross sectional area of cardiac chambers in front to back dimension--approximate
Frequency	80/min	Number of cycles per minute for chest and abdominal pressure
Duty cycle	0.5	Fraction of cycle time for chest compression
f_{tp}	0—1.0	Thoracic pump factor (0.75 = adult, 0.25 = child, 1.0 = emphysema, 0 = open chest)
Pinit	5 mmHg	Initial equilibrium pressure of arrested circulation
Fmax-chest	0—500 Nt	Maximum external force on sternum
x_0	0—4 cm	Effective compression threshold

Table 3: Elastic moduli of soft tissues.

Tissue	Approx. E (kPa)	Investigator	Year	Reference
Esophagus	15	Goyal	1971	[43]
Esophagus	15	Takeda	2002	[44]
Esophagus	25	Fan	2004	[45]
Lung	4	Matthews	1972	[46]
Lung	5	Hoppin	1975	[47]
Lung	1	Lai-Fook	1976	[48]
Lung	1	Karakaplan	1980	[49]
Skin	2	Barbenel	1973	[50]
Skin	22	Tong	1976	[51]
Mesentery	37	Chu	1972	[52]
Pulmonary artery	6	Patel	1960	[53]
Mean value	12			

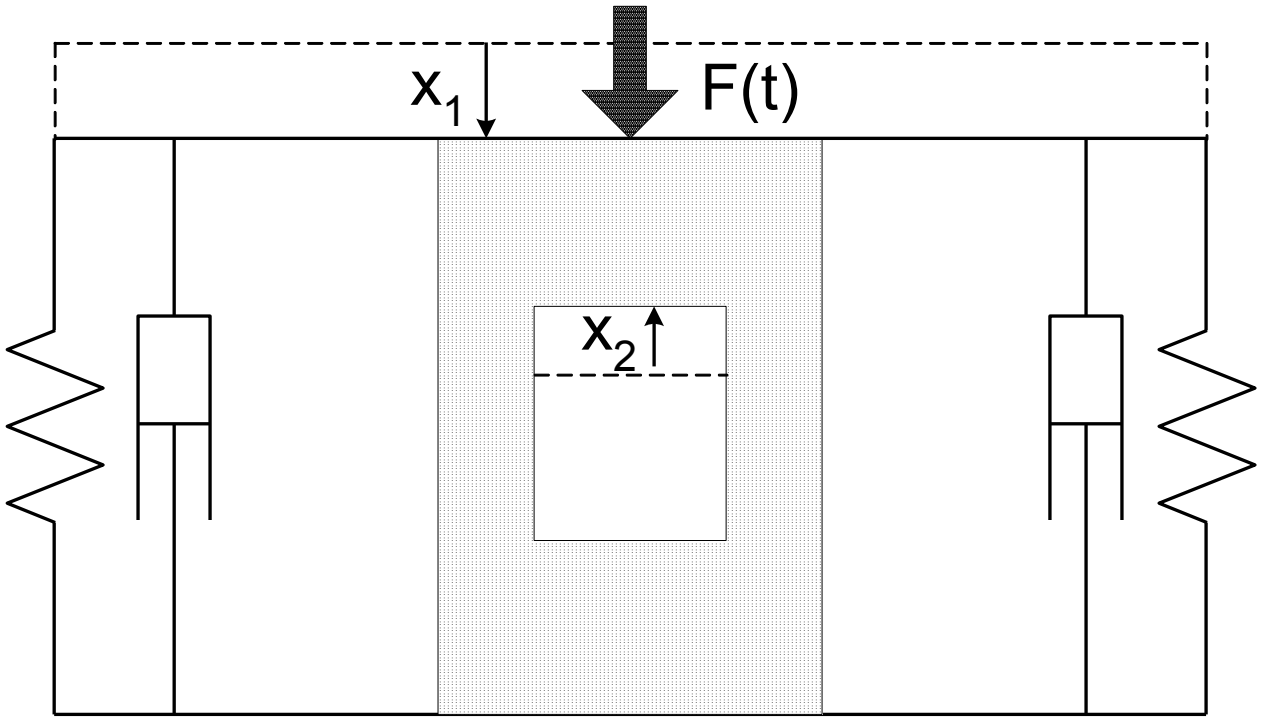

Figure 1: Model of chest wall, mediastinal tissues, and a representative cardiac chamber. The sketch represents a cross section of the chest; sternum on top. Outer springs and dampers represent the chest wall. F(t) is downward force applied to sternum. x_1 represents compression of the sternum and anterior chest wall. x_2 represents expansion of the cardiac chamber with blood. Stippling represents mediastinal soft tissue having Young's modulus of elasticity, E.

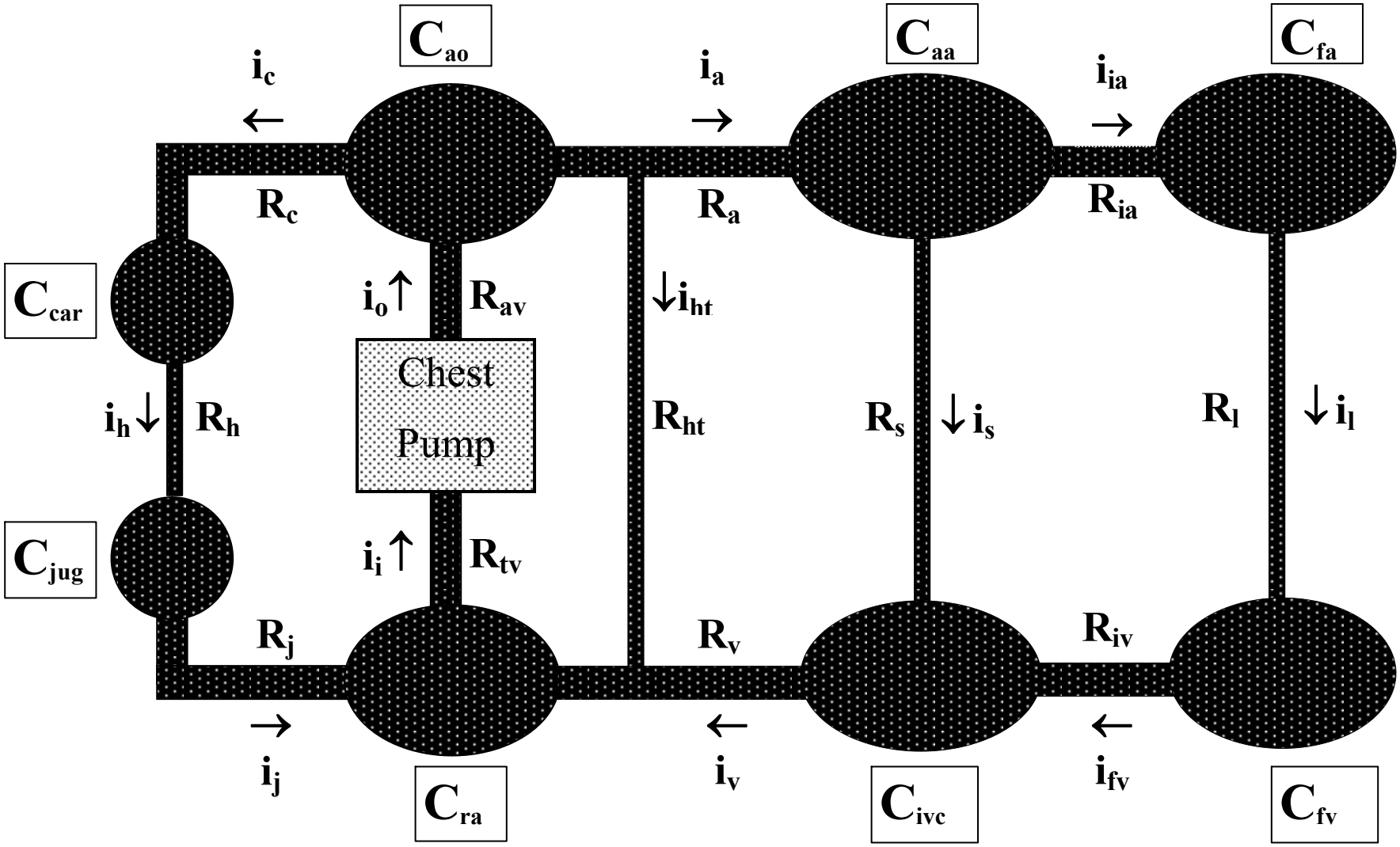

Figure 2. Model of the human circulatory system.

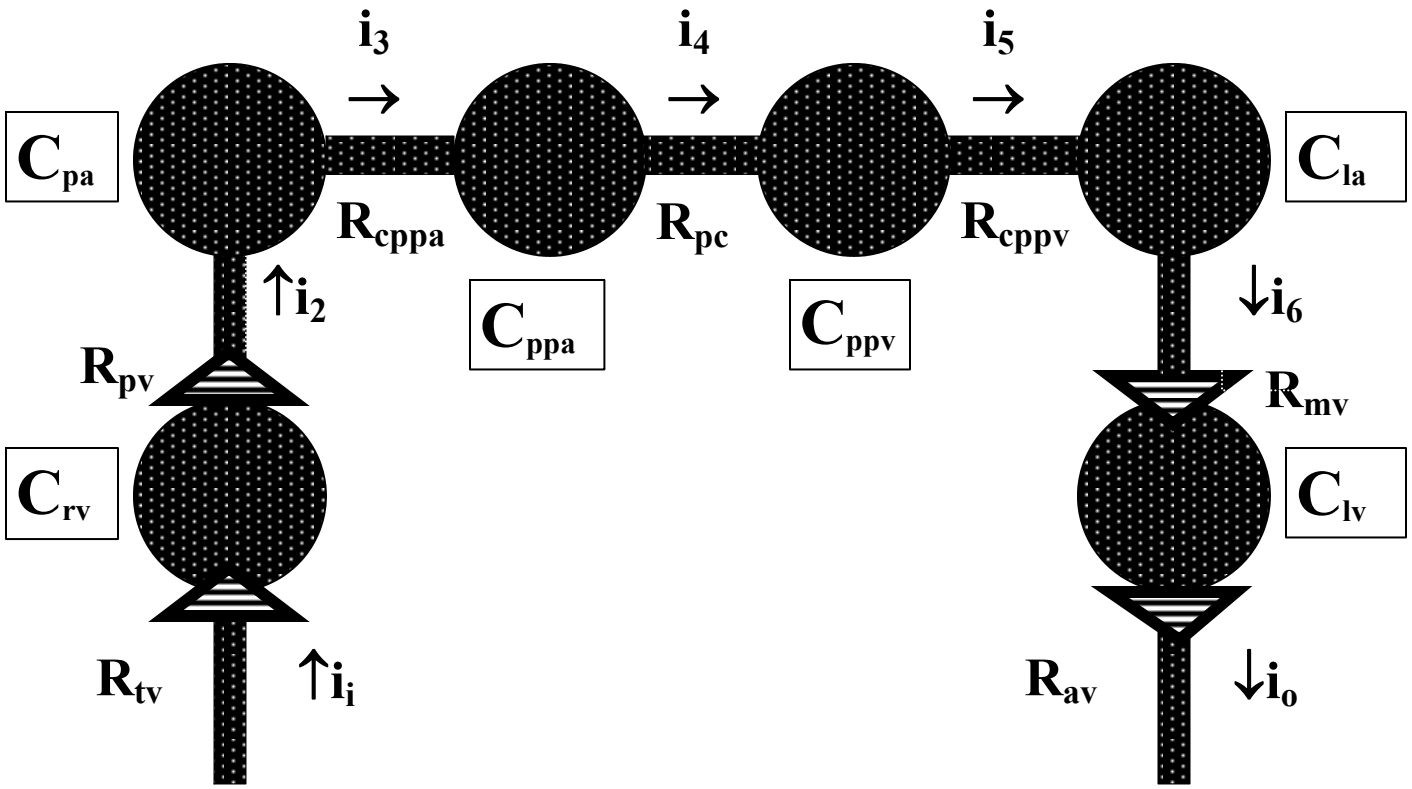

Figure 3. Detailed components within the chest. Triangles indicate heart valves.

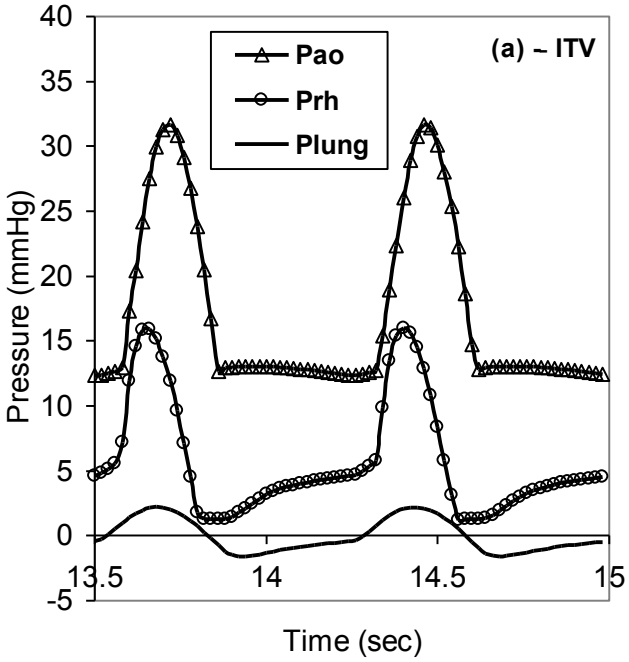

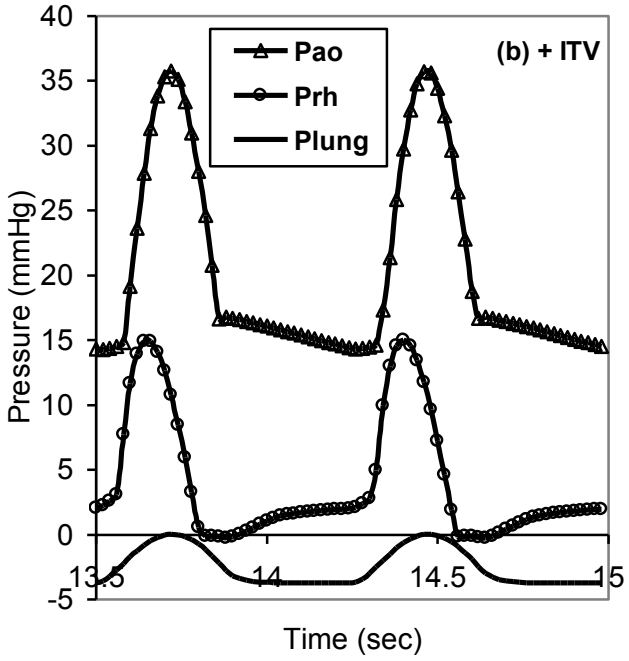

Figure 4. Cardiopulmonary pressures in simulations of CPR (a) without ITV, (b) with ITV. Thoracic pump factor 1.0. Effective compression threshold 2.0 cm. Maximal sternal displacement 5.1cm. Maximal chest compression force 400 Nt. Results show improved systemic perfusion pressure in (b).

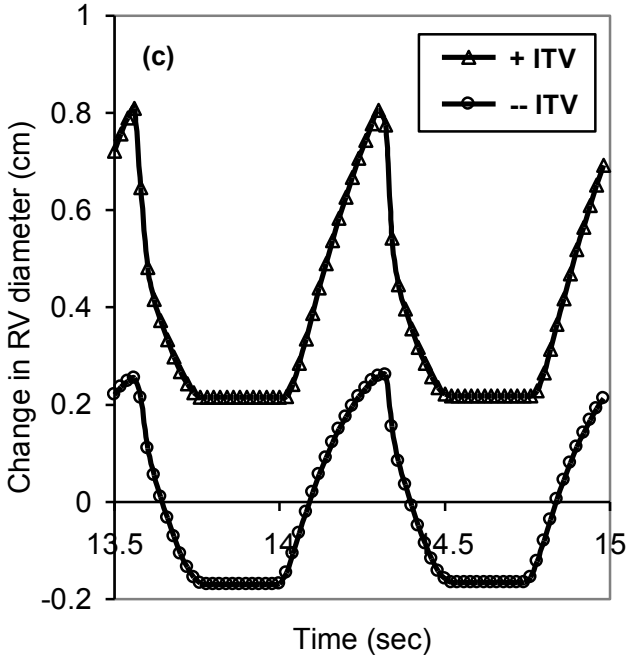

Figure 4(c). Changes in right ventricular dorsal-ventral diameter during standard CPR with and without an ITV. Thoracic pump factor 1.0. Effective compression threshold 2 cm. Peak chest compression force 400 Nt.

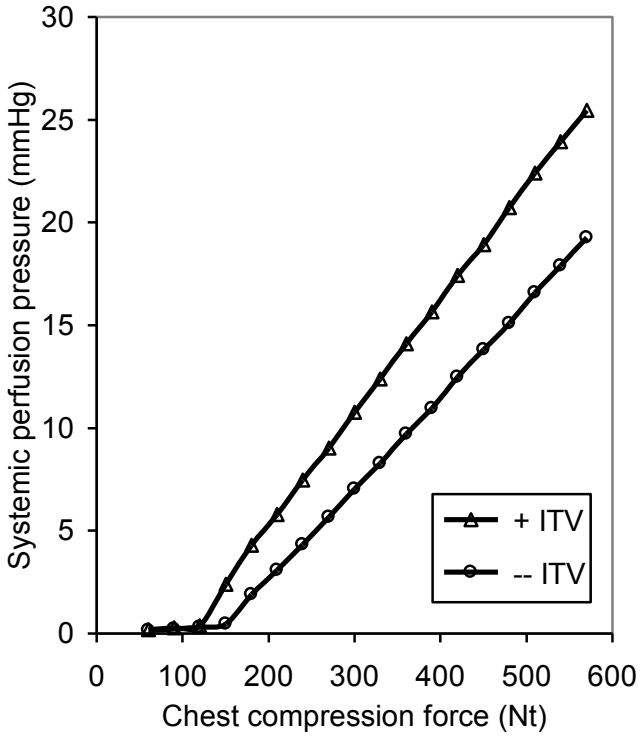

Figure 5. Systemic perfusion pressure during Standard CPR with and without an impedance threshold valve (ITV). Pure thoracic pump mechanism. The abscissa indicates peak compression force.

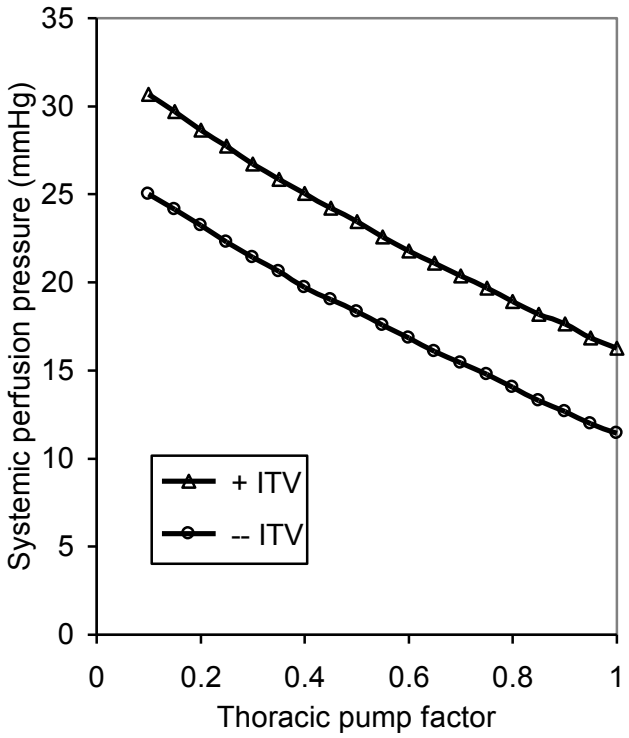

Figure 6. Systemic perfusion pressure during Standard CPR with 5.1 cm sternal deflection (400 Nt peak force) with and without an impedance threshold valve (ITV) for various chest pump mechanisms. The relative effect of the ITV is greater for thoracic pump CPR and less for cardiac pump CPR.

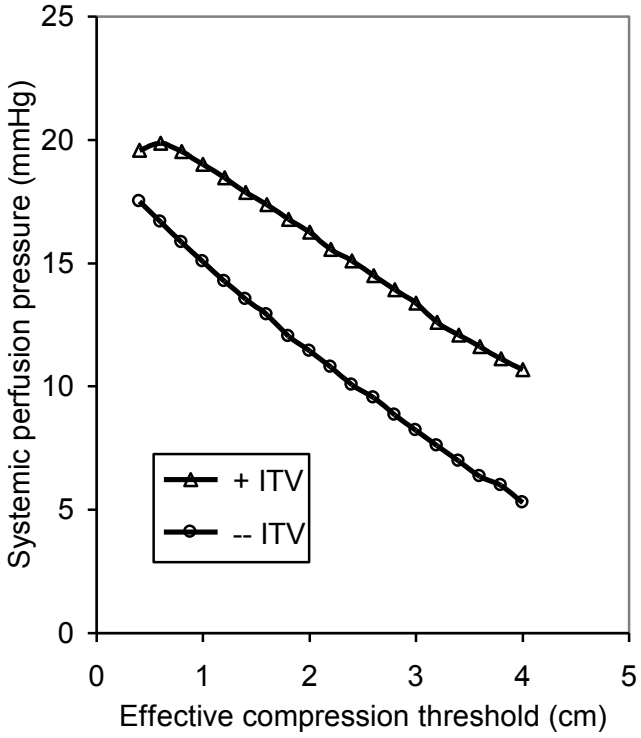

Figure 7. Systemic perfusion pressure during Standard CPR with 5.1 cm sternal deflection (400 Nt peak force) with and without an impedance threshold valve (ITV) for various effective compression thresholds. The relative effect of the ITV is greatest for larger compression thresholds. Here thoracic pump factor is 1.0.